

RF-CAVITY FOR THE X-RAY GENERATOR NESTOR

*V.P. Androsov¹, K.N. Chernov², A.M. Gvozd¹, I.M. Karnaukhov¹,
G.N. Ostreyko², I.K. Sedlyarov², Yu.N. Telegin^{1*}*

¹National Science Center "Kharkov Institute of Physics and Technology", 61108, Kharkov, Ukraine

²Budker Institute of Nuclear Physics (BINP), Novosibirsk, Russia

(Received March 13, 2007)

In the Kharkov Institute of Physics and Technology 225 MeV electron storage ring NESTOR is under development. The paper describes the design and parameters of a 700 MHz cavity that has been fabricated at BINP for the NESTOR RF-system. Now the low-power and vacuum tests of the cavity are under way at BINP. We present here the results of 3D simulations of the cavity with ANSYS code. The problem of multibunch instabilities in NESTOR is also discussed.

PACS: 29.20.Dh, 29.27.Bd

1. INTRODUCTION

Beam dynamics simulations in NESTOR, Compton scattering considered [1], have shown that for collision angle $\alpha=170^\circ$ and Nd laser ($\lambda_{laser}=1.06\mu\text{m}$) beam parameters available in the nearest future ($E_{laser}=20\mu\text{J/pulse}$, $f_{rep}=350\text{ MHz}$) an impact of Compton scattering on the electron beam is negligible and the electron beam parameters are dominated by intrabeam scattering and turbulent bunch lengthening. To overcome these effects and to obtain a bunch length which would match a pulse width of the commercially available Nd mode-locked laser

($\sim 7\text{ps}$) one has to apply the accelerating voltage of $\sim 300\text{ kV}$. This voltage will be provided with a single cell 700 MHz cavity.

In order to eliminate troubles concerned multibunch instabilities it would be reasonable to use a HOM-damped cavity like that designed for VEPP-5 damping ring project [2]. But from financial limitations we had to restrict ourselves to a common undamped cavity. The cavity shape and design are similar to that of the HOM-damped one. For the present time this cavity is under low-power and vacuum tests at BINP.

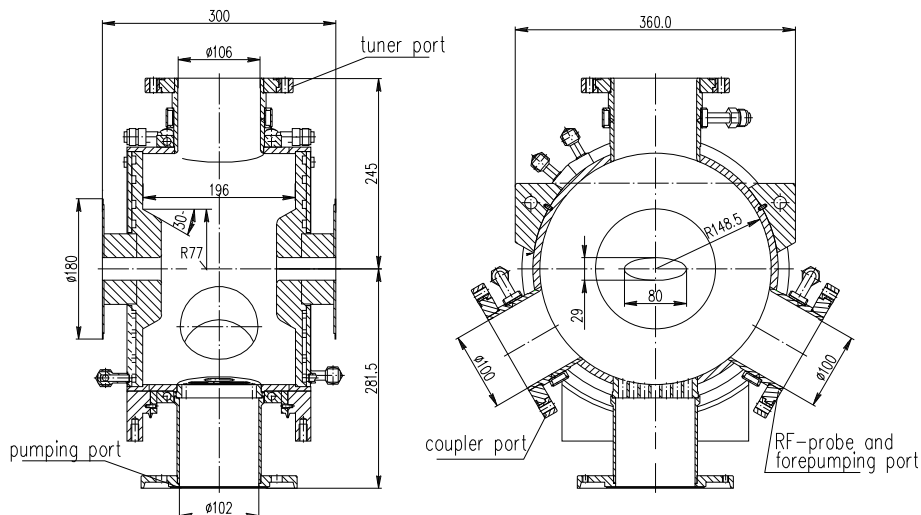


Fig.1. Cross sectional view of the cavity

2. CAVITY DESIGN AND PARAMETERS

Cavity design is presented in Fig.1. It is a cylindrical cavity with wide flat nosecones and short beam-pipes to meet stringent requirements to the

cavity length (30 cm). It has three ports placed equidistantly around the outer wall. The piston tuner moved with a step-motor is attached to the upper port. The coaxial coupler (70x20 mm, 75 Ω) with in-

*Corresponding author. E-mail address: telegin@kipt.kharkov.ua

ductive loop is connected to the cavity through one of the lower ports. The third port houses a field probe and a sleeve for connecting a fore-pumping unit. On the cavity bottom the fourth port without body-size hole but with pumping slots for ion pump is located. Cavity beam-pipes have an elliptical cross section, 80mm x 29mm, that matches that of the vacuum chamber, and they end with membranes, 180 mm diameter and 1mm thick, for welding.

Each sidewall is cooled through four concentric channels with rectangular cross section, 10x5 mm², machined into the wall and covered with a lid by brazing. The outer wall is cooled via two external circumferential channels which present the flat pipes brazed to the wall. Each port and the reciprocal flange are also provided with an external round channel. Additional cooling is provided for the tuner and coaxial coupler.

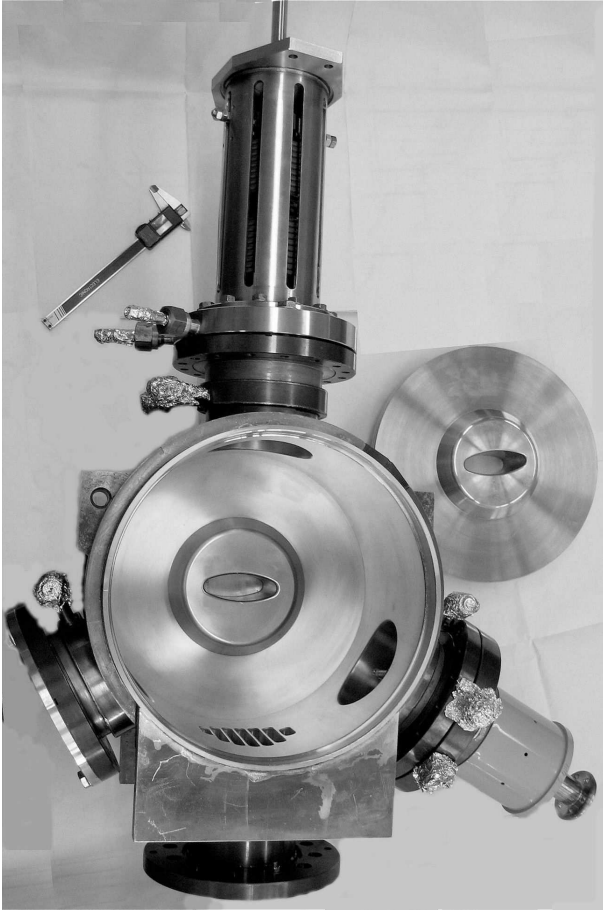


Fig.2. View of the cavity

The view of the cavity (with a mounted tuner) at fabrication stage before brazing the second side wall is given in Fig.2.

The main cavity parameters are presented in Table 1.

Table 1. RF-cavity parameters

Parameter	Value
Frequency, f_{rf} , MHz	699.3
Frequency range, Δf , MHz	± 0.8
Q-factor, Q	~ 20000
Shunt impedance, R_{sh} , M Ω	~ 4.5
Transit time factor, T	0.72
RF-voltage, V_0 , kV	250
Dissipated power, P_c , kW	15
Coupling factor, β	1.05–1.08

3. CAVITY SIMULATIONS

The preliminary simulations with SUPERFISH [3] of the axially-symmetric cavity with a cell shape similar to that of the real one have revealed 8 monopole modes below 2.8 GHz (the cut-off frequency of the 80 mm circular beam-pipe), which were easily identified as TM_{010} (fundamental mode), TM_{011} , TM_{012} , TM_{020} , TM_{021} , TM_{013} , TM_{022} and TM_{030} modes. Changing of the beam-pipe radius from 40 to 15 mm (the major and minor semi-axes of the beam-pipe cross section) led to the shift of fundamental mode frequency of about 10 MHz and to shifts of HOM frequencies in the range of 0 – 30 MHz. It should be noted that, at the same time, shunt impedance of the fundamental mode was increased by 20 percents; HOM impedances did not change essentially except that of TM_{021} mode. Longitudinal impedance of this mode was increased three times and reached 1.86 M Ω (1/4 of the fundamental mode shunt impedance).

The 3D simulations were performed with ANSYS code [4] by using the cavity model presented in Fig.3. Considering cavity symmetry relative to the median plane, only half-cell was modelled. The model includes a tuner port with a piston in neutral position, a coupler port and a probe/forepumping port. The last two ports have different lengths in the model according to the design of corresponding joints. The pumping slots at the bottom of the cavity were not taken into account.

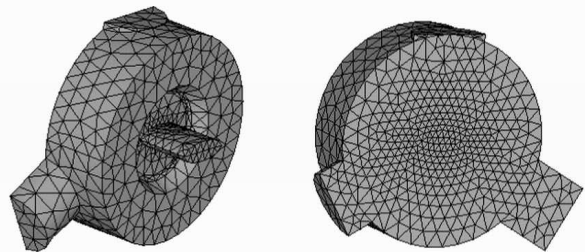


Fig.3. The NESTOR cavity model (half-cell) for 3D simulations with applied mesh

The ANSYS postprocessor outputs the following cavity parameters: mode frequency - f , Q-factor - Q and surface power losses - P_c . By using 'path operation' option one can calculate the following quantities:

– voltage drop along the beam axis:

$$V_0 = \left| \int_{-l/2}^{l/2} E_x dx \right|, \quad (1)$$

– transit time factor:

$$T = \frac{1}{V_0} \left| \int_{-l/2}^{l/2} E_x \exp(jkx) dx \right|, \quad (2)$$

– longitudinal (shunt) impedance:

$$R_{\parallel} = ZT^2 = \frac{V_0^2}{P_c} T^2. \quad (3)$$

Transverse impedances - R_{\perp} were calculated by using the following equation that is usually applied for derivation of R_{\perp} from experimental data in cold measurements [5]:

$$R_{\perp} = QZ_0 \left[j \int_V E_{\perp} \exp(jkx) dx - \int_V H_{\perp} \exp(jkx) dx \right]^2, \quad (4)$$

where $k = 2\pi f$ and $Z_0 = (\mu_0/\epsilon_0)^{1/2}$ is characteristic vacuum impedance. Sixty three resonances were found in the frequency range below 2.5 GHz. Parameters of the modes that can be of interest are presented in Table 2. The cavity model was built on basis of design drawings which take into account fabrication process with in-between frequency measurements and dimension corrections, so the fundamental frequency was found to be lower than the design value. Boundary conditions, presented in the second column, correspond to electric (E) or magnetic (M) wall on symmetry plane and beam-pipe flank.

Table 2. Cavity modes

f , MHz	BC	Q $\cdot 10^4$	R_{\parallel} , $M\Omega$	R_{\perp} , $M\Omega/m$	Mode origin
695.0	EE	2.96	7.31		TM_{010}
1008.3	ME	3.07	0.05	0.1	$TE_{111}^{(v)}$
1022.1	ME	3.16		1.2	$TE_{111}^{(h)}$
1017.9	ME	2.51	0.94		TM_{011}
1183.7	EE	3.95		2.7(v) 5.5(h)	$TM_{110}^{(1)}$
1185.6	EE	4.16		0.7(v) 20.4(h)	$TM_{110}^{(2)}$
1234.8	ME	3.55			$TE_{211}^{(1)}$
1257.5	ME	3.68			$TE_{211}^{(2)}$
1458.7	ME	3.04		43.3	$TM_{111}^{(v)}$
1491.0	ME	3.54		20.3	$TM_{111}^{(h)}$
1572.6	ME	3.40			TE_{311}
1606.7	EE	4.26			$TM_{210}^{(1)}$
1627.8	EE	4.65			$TM_{210}^{(2)}$
1668.3	EE	3.42			TM_{012}
1700.5	EE	3.41	0.02	5.5	$TE_{112}^{(h)}$
1717.2	EE	3.63	0.11	12.9	$TE_{112}^{(v)}$
1760.0	EE	4.60	0.24		TM_{020}
2009.5	ME	3.28	1.68		TM_{021}

The general notes are the following:

– each dipole mode splits into two modes - horizontal and vertical, as a rule;

– quadrupole modes split too, giving pairs with a similar field pattern but turned around the X-axis by 45° ;

– the pairs of modes with 3 azimuth variations and some other exotic modes appear;

– the longitudinal HOM-impedances well agree with SUPERFISH results, both reveal TM_{021} mode with $R_{\parallel}=1.7 M\Omega$ will be potentially dangerous.

The examples of calculated field patterns are given in Fig. 4 which illustrates dipole mode splitting when an azimuthal field pattern is influenced by the cavity ports (modes can not be defined as vertical and horizontal). For these modes two components of R_{\perp} , horizontal (h) and vertical (v), are presented in the tables.

In the Table 3 the obtained values R_{\parallel}/Q and R_{\perp}/Q for the most dangerous monopole and dipole modes are compared with those for the room-temperature cavities exploited in the course of many years in well-known electron storage rings. The table shows that NESTOR cavity has the highest R_{\parallel}/Q value of the fundamental mode (due to low cross section of beam-pipes). It has also the lowest R_{\parallel}/Q value of TM_{011} mode while the highest R_{\parallel}/Q value of TM_{021} .

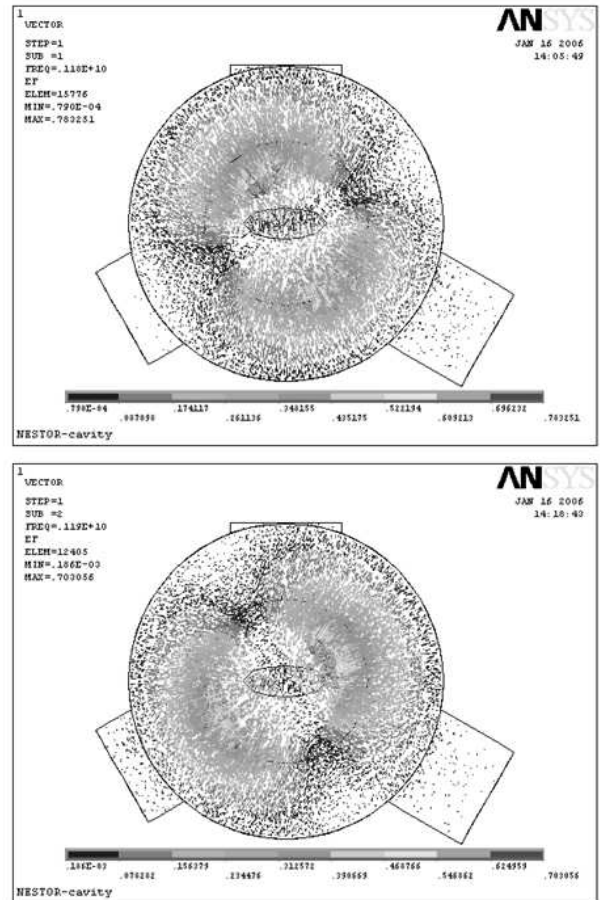


Fig. 4. Azimuthal distribution of the electric field for dipole modes 1183.7 MHz and 1185.6 MHz

Table 3. A comparison of the calculated factors R_{\parallel}/Q (R_{\perp}/Q) for the most prominent monopole (dipole) modes in different cavities

	SRS [6] (MAFIA 3D)		KEK-PF [7] (URMEL 2D)		ATF DR [8] ^a (MAFIA 3D)		NESTOR (ANSYS 3D)	
	f , MHz	$R_{\parallel}/Q(R_{\perp}/Q)$, Ω (Ω/m)	f , ^b MHz	$R_{\parallel}/Q(R_{\perp}/Q)$, Ω (Ω/m)	f , MHz	$R_{\parallel}/Q(R_{\perp}/Q)$, Ω (Ω/m)	f , MHz	$R_{\parallel}/Q(R_{\perp}/Q)$, Ω (Ω/m)
Monopole modes								
TM_{010}	498.8	195	500.1	175	724.7	169	695.0	247
TM_{011}	809.5	68	793.0	52	1044	62	1017.9	37
TM_{021}	1333.0	11	1371.0	9	1959	7	2009.5	51
Dipole modes								
$TM_{110}^{(1)}$	791.5	220	789.7	248	1152	263	1183.7	68(<i>v</i>) 139(<i>h</i>)
$TM_{110}^{(2)}$	797.1	255	792.6				1185.6	17(<i>v</i>) 490(<i>h</i>)
$TM_{111}^{(v)}$	1059.2	566	988.8	449	1349	726	1458.7	1424
$TM_{111}^{(h)}$	1059.3	568	989.8				1491.0	573

^aHOM-damped cavity, HOM-waveguides shorted.

^bExperimental values.

It should be noted that though the calculations for the ATF DR HOM-damped cavity were performed with 3D code MAFIA, the axially symmetric cavity was considered (if not taking into account HOM waveguides), so dipole mode splitting is not present in the table, like in the case of KEK PF cavity, simulated with 2D code URMEL. The comparison of R_{\perp}/Q for the dipole modes show that results for NESTOR cavity averaged over a number of split modes are within the range of R_{\perp}/Q values given for other cavities except that for $TM_{111}^{(h)}$ mode. The analysis of the axial field distribution shows that the large value of R_{\perp}/Q for this mode is accounted for by penetration of the field into a beam-pipe (vertical component of the electric field is high along the beam-pipe axis).

In the view of multibunch instabilities only modes trapped in the cavity are dangerous. Because the cavity shape is close to a pill-box and the beam-pipe cross section is elliptical, it isn't easy to calculate a cut-off frequency for beam-pipes. Simulations show that a number of trapped modes is large, and the problem of multibunch instabilities is vital for NESTOR ring.

The conservative estimates for coupled-bunch instabilities in NESTOR, obtained with traditional rigid-bunch approximation formulas [5], give the threshold bunch currents in the microampere range. These values are much lower than the designed value of 10 mA/bunch. We suppose to use the HOM tuning technique based on variation of cavity temperature [9] to cure these instabilities.

4. CONCLUSION

The 700 MHz accelerating cavity for the RF-system of electron storage ring NESTOR has been fabricated in BINP. Cavity simulations show that a large number of trapped modes with perceptible

coupling impedances can essentially complicate beam storing in NESTOR. The most dangerous are dipole modes (TM_{110} -like and TM_{111} -like).

REFERENCES

1. P. Gladkikh, I. Karnaukhov, A. Mytsykov et al. The Operation Modes of Kharkov X-ray Generator based on Compton Scattering NESTOR // *European Particle Accelerator Conf.* Luzern, Switzerland, 2004, p. 1428 – 1430.
2. N. Alinovsky, D. Bolkhovityanov, V. Dolgashev et al. RF system for VEPP-5 damping ring // *European Particle Accelerator Conf.* Stockholm, Sweden, 1998, p. 1799 – 1801.
3. J.H. Billen and L.M. Young. POISSON/ SUPER-FISH on PC Compatibles // *Particle Accelerator Conf.* Washington, USA, 1993, p. 790 – 792.
4. <http://www.ansys.com>
5. Y. Yamazaki, K. Takata, S. Tokumoto. Damping test of the higher-order modes of the re-entrant accelerating cavity // *IEEE Trans.*, 1981, NS28, p.2915–2917.
6. J.N. Corlett. *Higher order modes in the SRS 500 MHz accelerating cavities*: Preprint. Daresbury Laboratory, DL/SCI/P627A, 1989, 3 p.
7. N. Koseki, M. Izawa and Y. Kamiya. Development of a damped cavity with SiC beam duct // *Particle Accelerator Conf.* Dallas, USA, 1995, p.1791 - 1793.
8. S. Sakanaka, K. Kubo and T. Higo. Design of HOM damped cavity for the ATF damping ring // *Particle Accelerator Conf.* Dallas, USA, 1995, p.1027 - 1729.

9. H. Kobayakawa, M. Izagawa, S. Sakanaka and S. Tokumoto. Suppression of beam instabilities induced by accelerating cavities // *Rev.Sci.Instrum.*, 1989, v.60, p.1732–1735.

ВЧ-РЕЗОНАТОР ДЛЯ ГЕНЕРАТОРА РЕНТГЕНОВСКОГО ИЗЛУЧЕНИЯ НЕСТОР

В.П. Андросов, К.Н. Чернов, А.М. Гвоздь, И.М. Карнаузов, Г.Н. Острейко, И.К. Седяров, Ю.Н. Телегин

В НИЦ ХФТИ сооружается электронное накопительное кольцо НЕСТОР на энергию 225 МэВ. В работе описывается конструкция и приводятся параметры резонатора на 700 МГц, изготовленного в ИЯФ СО РАН им. Будкера для ВЧ-системы накопителя. В настоящее время резонатор проходит вакуумные испытания и радиотехнические измерения в ИЯФ. В работе также приводятся результаты 3D моделирования резонатора с помощью программы ANSYS. Обсуждается также проблема многоступенчатых неустойчивостей в накопителе НЕСТОР.

ВЧ-РЕЗОНАТОР ДЛЯ ГЕНЕРАТОРА РЕНТГЕНІВСЬКОГО ВИПРОМІНЮВАННЯ НЕСТОР

В.П. Андросов, К.М. Чернов, А.М. Гвоздь, І.М. Карнаузов, Г.М. Острейко, І.К. Седяров, Ю.М. Телегин

В НИЦ ХФТІ споруджується електронне накопичувальне кільце НЕСТОР на енергію 225 МеВ. У роботі описується конструкція та приводяться параметри резонатора на 700 МГц, виготовленого в ІЯФ СВ РАН ім. Будкера для ВЧ-системи накопичувача. У дійсний час резонатор проходить вакуумні випробування та радіотехнічні вимірювання в ІЯФ. У роботі також приводяться результати 3D моделювання резонатору за допомогою програми ANSYS. Обговорюється також проблема багатозгусткових нестійкостей у накопичувачі НЕСТОР.